Biosensors and Bioelectronics 56 (2014) 12–18

Contents lists available at ScienceDirect

Biosensors and Bioelectronics

journal homepage: www.elsevier.com/locate/bios

# Enzyme-free and label-free ultrasensitive electrochemical detection of DNA and adenosine triphosphate by dendritic DNA concatamer-based signal amplification

Shufeng Liu [a,*], Ying Lin [a], Tao Liu [a], Chuanbin Cheng [a], Wenji Wei [a], Li Wang [a,*], Feng Li [b,*]

[a] College of Chemistry and Molecular Engineering, Qingdao University of Science and Technology, Qingdao 266042, People's Republic of China
[b] College of Chemistry and Pharmaceutical Sciences, Qingdao Agricultural University, Qingdao 266109, People's Republic of China

ARTICLE INFO

*Article history:*
Received 18 November 2013
Received in revised form
14 December 2013
Accepted 26 December 2013
Available online 7 January 2014

*Keywords:*
Hybridization chain reaction
DNA hybridization
Electrochemical biosensor
Aptamer
ATP

ABSTRACT

Hybridization chain reaction (HCR) strategy has been well developed for the fabrication of various biosensing platforms for signal amplification. Herein, a novel enzyme-free and label-free ultrasensitive electrochemical DNA biosensing platform for the detection of target DNA and adenosine triphosphate (ATP) was firstly proposed, in which three auxiliary DNA probes were ingeniously designed to construct the dendritic DNA concatamer via HCR strategy and used as hexaammineruthenium(III) chloride (RuHex) carrier for signal amplification. With the developed dendritic DNA concatamer-based signal amplification strategy, the DNA biosensor could achieve an ultrasensitive electrochemical detection of DNA and ATP with a superior detection limit as low as 5 aM and 20 fM, respectively, and also demonstrate a high selectivity for DNA and ATP detection. The currently proposed dendritic DNA concatamer opens a promising direction to construct ultrasensitive DNA biosensing platform for biomolecular detection in bioanalysis and clinical biomedicine, which offers the distinct advantages of simplicity and cost efficiency owing to no need of any kind of enzyme, chemical modification or labeling.



## 1. Introduction

The development of ultrasensitive DNA biosensing platform capable of amplified detection toward trace amounts of target biomolecules is being greatly motivated by its potential applications in the early diagnosis and clinical treatment for some great diseases such as cancers (Lubin and Plaxco, 2010; Turner, 2013; Li et al., 2010a, 2010b; Wang et al., 2011; Kirsch et al., 2013; Sassolas et al., 2008). Electrochemical detection methods are particularly attractive due to its superior features of simple and portable instrumentation, rapid response and low cost (Ronkainen et al., 2010; Xiao et al., 2009; Hsieh et al., 2011; Odenthal and Gooding, 2007). Till now, different signal amplification strategies have been developed toward biomolecular detection for the sensitivity improvement (Comstock et al., 2011; Sorgenfrei et al., 2011; Qiu et al., 2013). They can be categorized into two distinct types: postamplification toward the signal produced by biorecognition events and target recycling by means of the operation of various nucleases. Examples of postamplification strategy include the use of enzymes (Patolsky et al., 2001; Liu et al., 2008), metal nanoparticles (Numnuam et al., 2008; Liao and Ho, 2009), and DNA bio-barcode (Stoeva et al., 2006; Li et al., 2010a, 2010b) as amplifying labels. However, these methods generally involve multiple assay steps, tedious labels and require the addition of many exogenous reagents. The target recycling methods via nucleases including endonuclease and exonuclease have also been widely employed for amplified detection toward various targets (Cao et al., 2012; Ji et al., 2012; Wu et al., 2011; Zuo et al., 2010; Freeman et al., 2011; Xu et al., 2012). Although sometimes the sensitivity is inspiring, these nuclease-based target recycling methods often suffer from the complexity of the experimental system. Also, false-positives may happen during the amplification process. Therefore, it is highly desirable to develop the enzyme-free, label-free and ultrasensitive detection method to satisfy the requirements for the profiling trace amounts of target biomolecules.

Recently, the hybridization chain reaction (HCR) strategy has become an attractive tool for signal amplification toward target detection owing to its significant advantages such as simple, cost-effective, isothermal and enzyme-free operation (Dirks and Pierce, 2004; Liu et al., 2013a; Xu et al., 2013; Chen et al., 2012a ). For example, Xia and co-workers proposed an ingenious supersandwich assay for DNA detection (Xia et al., 2010). In this assay, the formation of DNA supersandwich structure depends on the alternate hybridization between target DNA and signal probe in a

* Corresponding authors. Tel./fax: +86 532 84022681.
*E-mail addresses:* shufengliu77@yahoo.com (S. Liu), wangli@qust.edu.cn (L. Wang), lifeng@qust.edu.cn (F. Li).

0956-5663/$ - see front matter © 2014 Elsevier B.V. All rights reserved.
http://dx.doi.org/10.1016/j.bios.2013.12.066

stoichiometric ratio of 1:1, which limits the detection sensitivity. In order to address this issue, Chen and co-workers modified this approach by introducing an auxiliary DNA substitute for target DNA that can hybridize to two different regions of a signal DNA (Chen et al., 2011). The hybridization of auxiliary DNA and signal DNA can form a long DNA concatamer on the electrode surface. Thus, the formation of each long DNA concatamers is only involved into the use of one target DNA molecule, which correspondingly improves the detection limit toward target DNA. Now, the HCR strategy has been well developed as a general signal amplification method for the sensitive detection of DNA (Shimron et al., 2012; Chen et al., 2012b; Wang et al., 2011), protein (Zhang et al., 2012; Zhao et al., 2012) and small molecules (Yin et al., 2012; Yuan et al., 2011). Inspired by the HCR strategy for the construct of routine linear DNA concatamers, we envisioned that the dendritic DNA concatamers should be reasonably conceivable based on HCR by introducing three auxiliary DNA probes. It would be appealing for the fabrication of ultrasensitive DNA biosensing platform to further improve the detection sensitivity toward target DNA or DNA aptamer-related biomolecules.

Adenosine triphosphate (ATP), as a major energy currency of the cell, has been well known to play a critical role in the regulation of cellular metabolism and biochemical pathways in cell physiology. It has also been used as an indicator for cell viability and cell injury (Huizenga and Szostak, 1995; Wang et al., 2005; Llaudet et al., 2005; Zhou et al., 2011; Liu et al., 2013b). Thus, the determination of ATP is essential in biochemical study as well as clinic diagnosis. Herein, a novel enzyme-free and label-free ultrasensitive electrochemical DNA biosensing platform for DNA and ATP detection was developed, which employed the dendritic DNA concatamer as carriers for signal amplification. The dendritic DNA concatamer was formed by the HCR strategy between three introduced auxiliary DNA probes. With the use of hexaammineruthenium(III) chloride ($[Ru(NH_3)_6]^{3+}$, RuHex) as the electrochemical indicator, the ultrasensitive electrochemical detection toward DNA and ATP with a high selectivity could be realized. To the best of our knowledge, this should be the first attempt to fabricate dendritic DNA concatamer based on HCR strategy for signal amplification. It could offer a unique opportunity to construct ultrasensitive DNA biosensing platform for the detection of various biomolecules.

## 2. Experimental

### 2.1. Reagents and materials

Hexaammineruthenium(III) chloride ($[Ru(NH_3)_6]^{3+}$, RuHex) and 6-mercaptohexanol (MCH) were purchased from Sigma-Aldrich (St. Louis, MO, USA). Tris(2-carboxyethyl)phosphine (TCEP), Adenosine triphosphate (ATP), guanosine triphosphate (GTP), cytidine triphosphate (CTP), uridine triphosphate (UTP) and thymidine triphosphate (TTP) were purchased from Sangon Biotech Co., Ltd. (Shanghai, China). All other reagents were of analytical grade and purchased from Sinopharm Chemical Reagent Co. Ltd. (Shanghai, China). The HPLC-purified oligonucleotide sequences are purchased from Sangon Biotech. Co., Ltd. (Shanghai, China) and listed in Table S1. Human serum samples were kindly provided by the Qingdao Center Hospital. All solutions were prepared with ultrapure water obtained from a Milli-Q water purification system (Millipore Corp., Bedford, MA) with resistivity of 18.2 MΩ cm.

### 2.2. Immobilization of capture DNA probe on the electrode surface

The gold electrode was firstly polished with 0.05 μm alumina powder to obtain a mirror surface, followed by sonication in acetone and water for 5 min respectively. The gold electrode was then electrochemically cleaned in a 0.5 M $H_2SO_4$ solution within a potential window between −0.2 and +1.5 V at a scan rate of 100 mV $s^{-1}$ to remove any remaining impurities. The immobilization of capture probe DNA on the electrode was performed in 10 mM Tris–HCl solution (1 mM EDTA, 300 mM NaCl, 10 mM TCEP, pH 7.4) containing 0.5 μM capture probe DNA (CP1) or Anti-ATP aptamer fragment 1 (CP2) for 12 h at room temperature. Then, the electrode was immersed into 1 mM MCH for 1 h to remove the nonspecific DNA adsorption. The electrode surface was rinsed thoroughly and dried in nitrogen.

### 2.3. Target recognition and the assembly of dendritic DNA concatamer

The capture DNA modified electrode was then incubated into 50 μL of 10 mM Tris–HCl solution (pH 7.4, 1 mM EDTA, 300 mM NaCl, 1 mM $MgCl_2$) containing different concentrations of target DNA (TD1) or the mixture of different concentrations of ATP and 1 μM anti-ATP fragment 2 (TD2) for 2 h at room temperature. The electrode was then rinsed and dried. Afterward, the target recognized electrode was incubated into 50 μL of 10 mM Tris–HCl solution (pH 7.4, 300 mM NaCl, 1 mM $MgCl_2$) containing 1 μM AP1, 1 μM AP2 and 0.5 μM AP3 for 2 h. When the assembly was finished, the resulting electrode was again thoroughly rinsed and dried before electrochemical characterization.

### 2.4. Apparatus

Differential pulse voltammetry (DPV) and electrochemical impedance spectroscopy (EIS) were performed with a CHI 660D electrochemical workstation (CH Instruments, Shanghai, China). All electrochemical experiments were performed with a conventional three-electrode system comprising a gold working electrode, a platinum wire auxiliary electrode, and a Ag/AgCl reference electrode. The DPV measurements were conducted with the first incubation of the assembled electrode into 10 mM Tris–HCl solution (pH 7.4) containing 50 μM RuHex for 20 min. After that, the resulting electrode was thoroughly rinsed and dried, and recorded for DPV responses in 10 mM Tris–HCl solution (pH 7.4) by using a potential window of 0 to −0.5 V. The EIS experiments were measured in 1 mM $Fe(CN)_6^{3-/4-}$ solution containing 0.5 M KCl with the frequency range from 0.1 Hz to 10 kHz. The chronocoulometry measurements were taken over a range of 0 V to −0.35 V to 0 V at a pulse period of 250 ms with the RuHex as an indicator. Before electrochemical measurements, the electrolyte solution should be thoroughly purged with high purity nitrogen for about 20 min, to avoid the interference from the reduction of oxygen.

## 3. Results and discussion

### 3.1. Design principle of DNA biosensing platform

The DNA biosensing platform based on dendritic DNA concatamer is schematically demonstrated in Fig. 1. In order to achieve the one-step automatic formation of dendritic DNA concatamers for signal amplification, three auxiliary DNA probes, named AP1, AP2 and AP3, are ingeniously designed. The AP1 can hybridize with two different regions of the AP2. As a result, a cascade of hybridization events between alternating AP1 and AP2 will lead to the formation of a typical one-dimensional linear DNA concatamer, which contains the dangling fragments (The fragments at the 5′ end of AP1 or AP2, respectively) flanked on the concatamer. The AP3 is designed that possesses two different base sequence regions. The base sequence at the 5′ end of AP3 is complementary

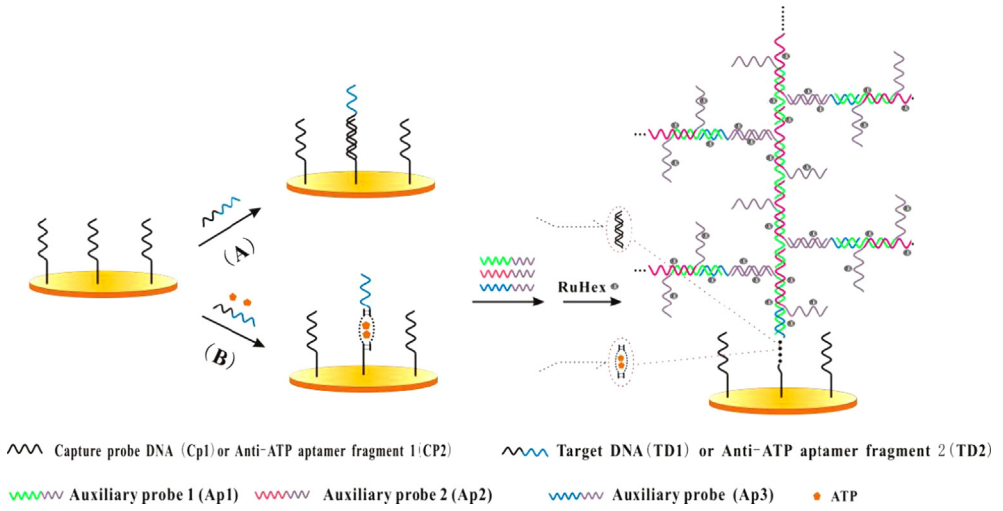


**Fig. 1.** The schematic illustration of DNA biosensor fabrication based on dendritic DNA concatamer for the detection of target DNA (A) and ATP (B).

with the dangling fragment of AP1 or AP2, and the region at the 3′ end of AP3 possesses the same base sequence with that at the 3′ end of target DNA (TD1) or anti-ATP aptamer fragment 2 (TD2), which can hybridize with the fragment at the 3′ end of AP1. The AP3 is thus considered to play a bridge role to further trigger the alternate hybridization between AP1 and AP2 across the side chain direction. Thus, a three-dimensional dendritic DNA concatamer will be automatically formed in the case that the AP1, AP2 and AP3 are simultaneously added in the sensing system. In the case of target DNA (TD1) detection, one terminus of the TD1 can hybridize with the immobilized CP1 on the electrode, and the other terminus can hybridize with dendritic DNA concatamers via AP1. Thus the dendritic DNA concatamer can be connected to the immobilized CP1 on the electrode surface via TD1. Since the DNA backbone is negatively charged, myriad RuHex can bind to the dendrtic DNA concatamers through electrostatic interaction and eventually result in significantly amplified electrochemical signals for TD1 detection. Furthermore, the proposed dendritic DNA concatamer-based signal amplification strategy can also be extended for aptasensor fabrication. With the ATP as an example, the ultrasensitive detection of ATP can be achieved by using a split aptamer strategy (Chen and Zeng, 2013; Liu et al., 2010). The anti-ATP aptamer is split into two fragments. The anti-ATP aptamer fragment 1 is immobilized on the electrode as capture probe (CP2) and the anti-ATP aptamer fragment 2 (designated as TD2) contains a complementary region with AP1 at the 3′ terminus. In the presence of ATP, these two dissociated fragments would assemble to form intact structures by binding ATP. Furthermore, the dendritic DNA concatamers can be linked onto the electrode via AP1.

### 3.2. *Electrochemical characterization of fabricated DNA biosensor*

RuHex cation has been well explored as an electrochemical indicator to quantitatively bind to the phosphate backbone of DNA via electrostatic interaction. Usually, more RuHex binding to DNA can induce greater electrochemical signal. The feasibility of the developed electrochemical DNA biosensor for target DNA (TD1) detection was firstly examined and shown in Fig. 2. In the absence of TD1, a small reduction peak could be observed (Fig. 2a), due to the electrostatic binding of small amount of RuHex to CP1. After hybridized with TD1, only a slightly increased peak current was obtained owing to the binding of some more RuHex cations onto the CP1 and TD1 (Fig. 2b). When the solution containing 1.0 μM AP1 and 1.0 μM AP2 was dripped on the surface of the electrode, the linear DNA concatamers formed by AP1 and AP2 could be

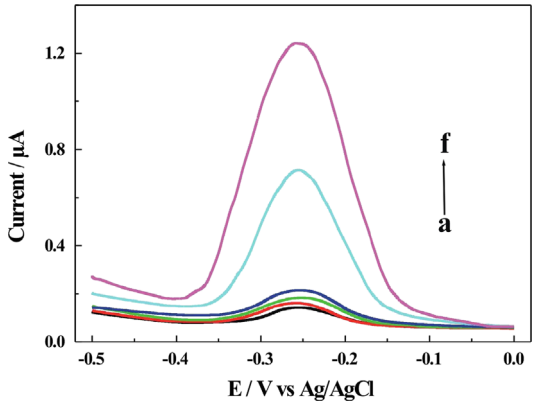


**Fig. 2.** DPV responses of the gold electrode assembled with different oligonucleotides: (a) CP1, (b) CP1+TD1, (c) CP1+AP1+AP2, (d) CP1+AP1+AP2+AP3, (e) CP1+TD1+AP1+AP2, and (f) CP1+TD1+AP1+AP2+AP3. The concentration of TD1 is 1 pM. The concentrations of AP1, AP2 and AP3 are 1 μM, 1 μM and 0.5 μM, respectively.

firmly immobilized on the gold electrode. Thus a large number of RuHex binding to DNA concatamers produced a remarkable amplified electrochemical signal (Fig. 2e). Furthermore, the introduction of 0.5 μM AP3 in the above solution containing AP1 and AP2 resulted in the formation of dendritic DNA concatamers accompanied by binding of more amounts of RuHex, which produced a further largely increased electrochemical signal (Fig. 2f). In the absence of TD1, although the linear DNA concatamers or the dendritic DNA concatamers might be produced in the solution by the self-assembly of AP1 and AP2 or AP1, AP2 and AP3, respectively, they could not be effectively linked to the electrode surface. Thus, still only small reduction peaks were obtained (Fig. 2c and d), due to the nonspecific adsorption of formed DNA concatamers on the electrode surface. Therefore, the current dendritic DNA concatamer-based signal amplification strategy was hopeful to offer an ultrahigh sensitivity for the assay of DNA or DNA-related targets.

The DNA biosensor fabrication process has also been confirmed by EIS measurements (Fig. S1 in the Supplementary material). The EIS of bare electrode only exhibited a very small semicircular domain (curve *a* in Fig. S1), indicating a fast charge-transfer process. After immobilization of CP1 and MCH on the electrode, a big semicircle with Rct value of about 3777 Ω could be observed (curve *b* in Fig. S1), indicating an increase of the charge transfer resistance. It could be explained by that the negatively charged

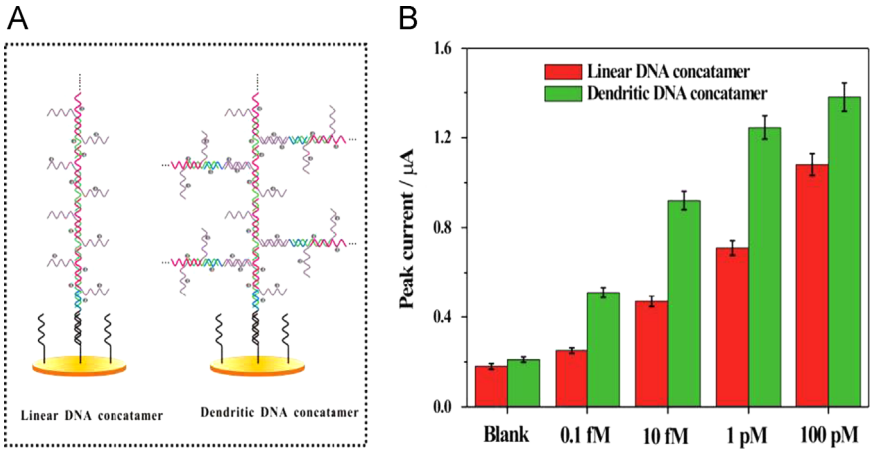


**Fig. 3.** (A) The schematic illustration of signal amplification by linear or dendritic DNA cocatamer. (B) Bar chart of DPV peak currents recorded for the DNA biosensor fabricated with linear DNA concatamer (red bars) and dendritic DNA concatamer (green bars) toward different concentrations of TD1. The error bars are standard deviations of three repetitive measurements. (For interpretation of the references to color in this figure legend, the reader is referred to the web version of this article.)

phosphate backbone of assembled capture DNA prevented the diffusion of $[Fe(CN)_6]^{3-/4-}$ toward the electrode surface. In the presence of TD1, the Rct value was only slightly increased (curve *c* in Fig. S1). With the introduction of AP1 and AP2, the linear DNA concatamer formed on the electrode by alternative hybridization of AP1 and AP2 induced a largely increased Rct value of about 9504 Ω (Curve *e* in Fig. S1). Furthermore, the introduction of AP3 yielded a more remarkably increased impedance change with the Rct value of about 16543 Ω (Curve *f* in Fig. S1), indicating the formation of dendritic DNA concatamer, repelling the negatively charged redox species more strongly. It should be noted that only a small change of the diameter of semicircle compared with that of CP1 modified electrode was observed in the case of non-complementary target DNA as an alternative (curve *d* in Fig. S1). The impedance experiments demonstrated that the dendritic DNA concatamer had been successfully created by the HCR between three auxiliary DNA probes. It also provided an effective tool for DNA detection by EIS experiments based on the signal amplification of dendritic DNA concatamer.

### 3.3. Optimization of self-assembled DNA nanostructures

The assembly density of capture DNA probe on the electrode surface would have an important effect on the performance of electrochemical DNA biosensor. The immobilization concentration of CP1 was firstly optimized based on the electrochemical response toward TD1 detection (Fig. S2A in the Supplementary material). It could be found that the CP1 concentration of 0.5 μM could achieve the better electrochemical response than that at other concentrations. The surface coverage of assembled CP1 under the optimum condition had also been determined on the basis of Tarlov's method by chronocoulometry (Steel et al., 1998). It was estimated to be 4.43 $(\pm 0.21) \times 10^{-12}$ mol cm$^{-2}$ based on three independent experiments. The higher CP1 concentration can increase the assembly density on the electrode surface, but it may restrict the hybridization efficiency of TD1 and further accessibility of the dendritic DNA concatamers toward the DNA hybrids on the electrode surface (Zhang et al., 2006).

The signal amplification of built electrochemical DNA biosensor is based on the generated dendritic DNA concatamer via the cascaded hybridization events between three auxiliary probes (AP1, AP2 and AP3). Thus, the concentrations of the auxiliary probes and the hybridization time play the important role for the assembly of dendritic DNA concatamer. The alternate hybridization between AP1 and AP2 endowed the formation of linear DNA concatamers. The same concentration of AP1 and AP2 were used and optimized from 0 to 1.5 μM (Fig. S2B in the Supplementary material). The concentration of 1.0 μM of AP1 and AP2 could reach the maximum electrochemical response. Thus the concentration of AP1 and AP2 was chosen as 1.0 μM. The AP3 was used to trigger the alternate hybridization between AP1 and AP2 across the side chain direction of linear DNA concatamers. Its concentration was also optimized while keeping the concentrations of AP1 and AP2 constant (1.0 μM) (Fig. S2C in the Supplementary material). It could be seen that the electrochemical response toward 1 pM TD1 increased as the concentration of AP3 up to 0.5 μM and then decreased with the further increase of AP3 concentration. The decrease of electrochemical response observed at a higher AP3 concentration may be explained that a higher concentration of AP3 would benefit the HCR process along the side chain of dendritic DNA concatamers, bringing the constraints for the accessibility DNA concatamers toward the TD1 on the electrode surface. Thus, the optimized AP3 concentration was chosen as 0.5 μM. The effect of hybridization time was also examined (Fig. S2D in the Supplementary material). The peak current increased as the hybridization time changed from 0 to 120 min. Then the peak current did not increase obviously as the hybridization time extended to 150 min. Therefore, the optimum hybridization time was chosen as 120 min.

### 3.4. Sensitivity of proposed electrochemical DNA biosensor

The signal amplification effect for TD1 detection by current dendritic DNA concatamer (assembly from AP1, AP2 and AP3) was further compared with that by the typical linear DNA concatamer (assembly from AP1 and AP2). It could be seen from Fig. 3 that the typical strategy based on linear DNA concatamer only showed a detection limit of about 0.1 fM for TD1. In contrast, the electrochemical response to TD1 by dendritic DNA concatamer at the same concentration was significantly higher than that by linear DNA concatamer. After subtracting the background response of the blank solution, the peak current obtained with the dendritic DNA concatamer for 0.1 fM TD1 was about 3.3 times higher than that by linear DNA concatamer, showing the remarkable amplification performance of dendritic DNA concatamer. Also, the signal amplification effects by dendritic DNA concatamer compared with linear DNA concatamer were more evident with the decrease of TD1 concentration. It could be observed that the peak current obtained with the dendritic DNA concatamer for 100 pM TD1 was only 0.3 times higher than that by linear DNA concatamer. It could be

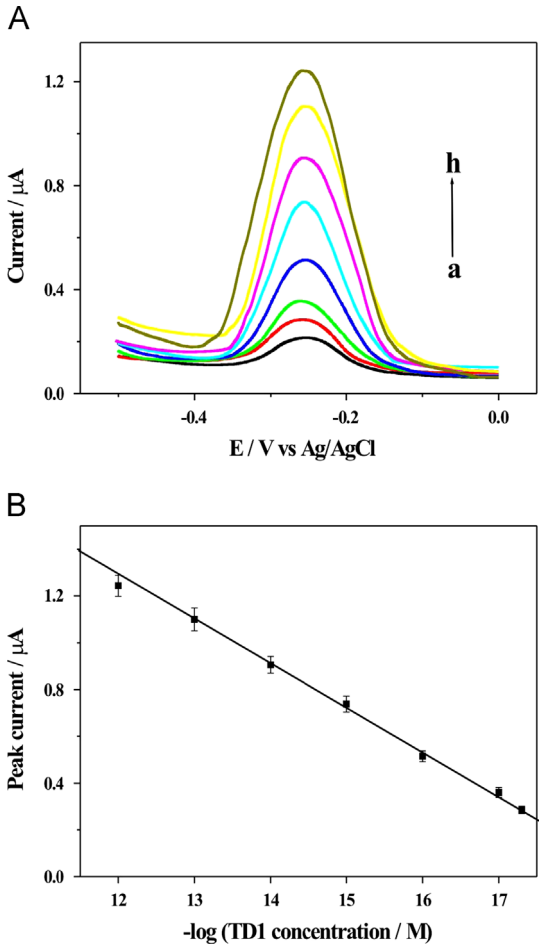


**Fig. 4.** (A) DPV responses of fabricated DNA biosensor toward the detection of different concentrations of TD1: (a) 0 M, (b) 5 aM, (c) 10 aM, (d) 100 aM, (e) 1 fM, (f) 10 fM, (g) 100 fM, (h) 1 pM. (B) The linear plots of peak currents vs the negative logarithm of TD1 concentrations. Error bars showed the standard deviation of three experiments.

explained that the steric hindrance effect of the dendritic DNA concatamer for TD1 recognition was more evident than that of linear DNA concatamer, especially at a relatively high concentration of TD1 (Ji et al., 2012). However, the dramatic signal amplification efficiency by dendritic DNA concatamer toward low abundance DNA implied the sensitivity improvement of the fabricated DNA biosensor.

Furthermore, the fabricated biosensor based on dendritic DNA concatamer was used to explore the sensitivity for TD1 detection. As shown in Fig. 4A, the DPV peak current increased when the concentration of TD1 was raised from 0 to 1 pM, indicating that the assembly of dendritic DNA concatamer on the electrode surface was dependent on the concentration of target DNA. Fig. 4B showed that the DPV peak currents of fabricated DNA biosensor exhibited a good linear correlation to the negative logarithm of the concentrations of the TD1 ranging from 5 aM to 1 pM with a linear correlation coefficient of 0.9988. The directly measured detection limit was as low as 5 aM, providing superior or comparable detection sensitivity compared with most of reported methods (see Table S2 in the Supplementary material).

### 3.5. Selectivity and stability of the fabricated DNA biosensor

The specificity of the proposed detection method was further investigated by using four kinds of DNA sequences, including complementary target DNA, single-base mismatched DNA, two-base mismatched DNA, and non-complementary DNA at the same concentration of 1 pM. As shown in Fig. 5, the DPV peak current for one-base mismatched DNA and two-base mismatched DNA was about 33.7% and 22.1% of that for perfect target at the same concentration, respectively. The noncomplementary target DNA shows almost the same response with the blank solution. Thus, this method exhibited a good performance to discriminate perfect complementary target and the base mismatched targets and great potential for single nucleotide polymorphism analysis. We further challenged the detection toward target DNA spiked in relatively complex biological matrix (1:5 dilution of human serum). Comparable responses were obtained for the detection of target DNA in both buffer and real samples (Fig. S3 in the Supplementary material), indicating the potential for real analytical application.

The stability for the CP1 modified electrode has also been checked. Three independent experiments demonstrated that the CP1 modified electrode could retain about 94.7% of its initial response toward TD1 after its storage in the refrigerator at 4 °C for 10 days, showing a relatively robust stability of the CP1 modified electrode.

### 3.6. Sensitivity and selectivity for electrochemical detection of ATP

Furthermore, the optimized sensing system was applied for the quantitative detection of ATP by using the split aptamer strategy. Fig. 6A showed that the DPV peak current increased with the increase of ATP concentration from 0 to 10 nM. The DPV peak current was found to exhibit a good linear correlation to the negative logarithm of the concentrations of the ATP ranging from 20 fM to 10 nM with a linear correlation coefficient of 0.9977. The directly measured detection limit for ATP was as low as 20 fM, providing the superior or comparable detection sensitivity compared with most of reported methods (see Table S3 in the Supplementary material).

The specificity of the sensing system for ATP detection was also evaluated by using four ATP analogues including guanosine triphosphate (GTP), cytidine triphosphate (CTP), uridine triphosphate (UTP), and thymidine triphosphate (TTP). As shown in Fig. 6C, significant DPV response was observed only in the presence of ATP. Whereas other tested analogues showed almost the same background values, indicating the sufficient selectivity for ATP detection, which could be ascribed to the high selectivity of the anti-ATP aptamer to its target.

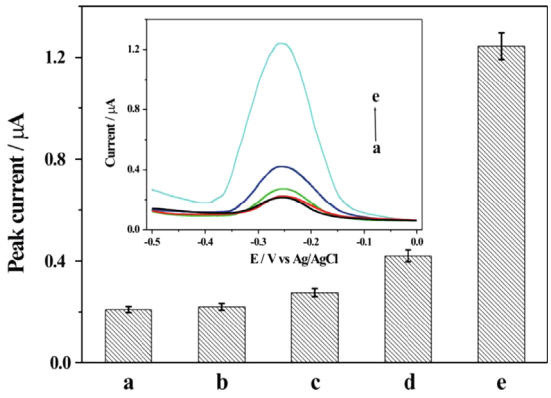


**Fig. 5.** The bar chart of the DPV responses toward the blank (a) and the four various DNA sequences including (b) non-complementary, (c) two-base mismatched, (d) single-base mismatched, and (e) complementary target DNA. The concentrations of various DNA sequences were 1 pM. The error bars represent the standard deviation of three repetitive measurements. The inset shows the corresponding DPV responses.

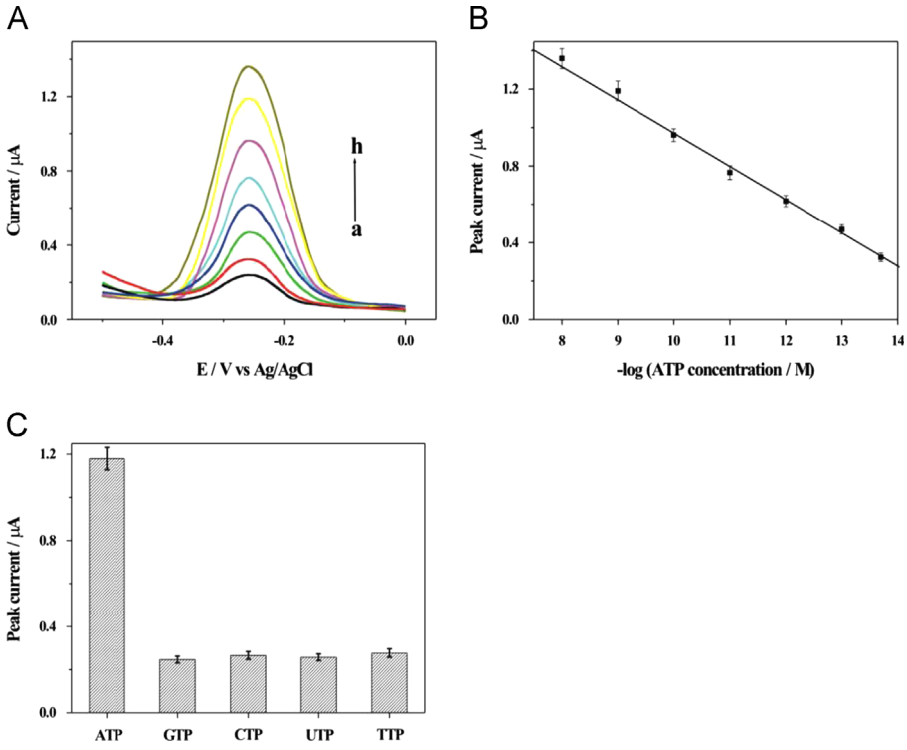


**Fig. 6.** (A) DPV responses corresponding to the detection of different concentrations of ATP: (a) 0 M, (b) 20 fM, (c) 100 fM, (d) 1 pM, (e) 10 pM, (f) 100 pM, (g) 1 nM, (h) 10 nM. (B) Linear relationship between DPV peak current and the negative logarithm of ATP concentration from 20 fM to 10 nM. (C) Selectivity of the proposed electrochemical DNA biosensor to ATP, GTP, CTP, UTP and TTP at 1 nM, respectively. Error bars are obtained based on four independent measurements.

## 4. Conclusion

We have demonstrated an enzyme-free and label-free ultrasensitive electrochemical DNA biosensing platform for specific detection of target DNA and ATP. Three auxiliary DNA probes are ingeniously designed to construct the dendritic DNA concatamer as carrier of electroactive RuHex cations for signal amplification. A detection limit as low as 5 aM and 20 fM toward target DNA and ATP, respectively, could be achieved. The developed ultrasensitive electrochemical DNA biosensor, no need of any kind of enzyme, label or sophisticated equipment, has a great potential in the area of DNA diagnostics and clinical analysis. Meanwhile, it should be easily combined with other analytical techniques for example fluorescence, electrochemiluminence, etc., and could be extended for the detection toward a wide spectrum of target biomolecules.

## Acknowledgements

This work was funded by the National Natural Science Foundation of China (Nos. 21005043, 21375072 and 21175076), the Basic Research Program of Qingdao (No. 13-1-4-214-jch), and the Science Foundation of China Postdoctor (No. 2012M511537).

## Appendix A. Supplementary material

Supplementary data associated with this article can be found in the online version at http://dx.doi.org/10.1016/j.bios.2013.12.066.

## References

Cao, Y., Zhu, S., Yu, J., Zhu, X., Yin, Y., Li, G., 2012. Anal. Chem. 84, 4314–4320.
Chen, J., Zeng, L., 2013. Biosens. Bioelectron. 42, 93–99.
Chen, X., Lin, Y.H., Li, J., Lin, L.S., Chen, G.N., Yang, H.H., 2011. Chem. Commun. 47, 12116–12118.
Chen, X., Hong, C.Y., Lin, Y.H., Chen, J.H., Chen, G.N., Yang, H.H., 2012a. Anal. Chem. 84, 8277–8283.
Chen, Y., Xu, J., Su, J., Xiang, Y., Yuan, R., Chai, Y., 2012b. Anal. Chem. 84, 7750–7755.
Comstock, M.J., Ha, T., Chemla, Y.R., 2011. Nat. Methods 8, 335–340.
Dirks, R.M., Pierce, N.A., 2004. Proc. Nat. Acad. Sci. U.S.A 101, 15275–15278.
Freeman, R., Liu, X., Willner, I., 2011. Nano Lett. 11, 4456–4461.
Hsieh, K., White, R.J., Ferguson, B.S., Plaxco, K.W., Xiao, Y., Soh, H.T., 2011. Angew. Chem. Int. Ed. 50, 11176–11180.
Huizenga, D.E., Szostak, J.W., 1995. Biochemistry 34, 656–665.
Ji, H., Yan, F., Lei, J., Ju, H., 2012. Anal. Chem. 84, 7166–7171.
Kirsch, J., Siltanen, C., Zhou, Q., Revzin, A., Simonian, A., 2013. Chem. Soc. Rev. 42, 8733–8768.
Li, D., Song, S.P., Fan, C.H., 2010a. Acc. Chem. Res. 43, 631–641.
Li, H., Sun, Z., Zhong, W., Hao, N., Xu, D., Chen, H.Y., 2010b. Anal. Chem. 82, 5477–5483.
Liao, W.C., Ho, A.H., 2009. Anal. Chem. 831, 2470–2476.
Liu, G., Wan, Y., Gau, V., Zhang, J., Wang, L., Song, S., Fan, C., 2008. J. Am. Chem. Soc. 130, 6820–6825.
Liu, P., Yang, X., Sun, S., Wang, Q., Wang, K., Huang, J., Liu, J., He, L., 2013a. Anal. Chem. 85, 7689–7695.
Liu, S., Wang, Y., Zhang, C., Lin, Y., Li, F., 2013b. Chem. Commun. 49, 2335–2337.
Liu, Z., Hu, L., Li, H., Zhu, S., Xu, G., 2010. Chem. Euro. J. 16, 13356–13359.
Llaudet, E., Hatz, S., Droniou, M., Dale, N., 2005. Anal. Chem. 77, 3267–3273.
Lubin, A.A., Plaxco, K.W., 2010. Acc. Chem. Res. 43, 496–505.
Numnuam, A., Chumbimuni–Torres, K.Y., Xiang, Y., Bash, R., Thavarungkul, P., Kanatharana, P., Pretsch, E., Wang, J., Bakker, E., 2008. J. Am. Chem. Soc. 130, 410–411.
Odenthal, K.J., Gooding, J.J., 2007. Analyst 132, 603–610.
Patolsky, F., Lichtenstein, A., Willner, I., 2001. Nat. Biotechnol. 19, 253–257.
Qiu, L., Qiu, L., Wu, Z.S., Shen, G., Yu, R.Q., 2013. Anal. Chem. 85, 8225–8231.
Ronkainen, N.J., Halsall, H.B., Heineman, W.R., 2010. Chem. Soc. Rev. 39, 1747–1763.
Sassolas, A., Leca-Bouvier, B.D., Blum, L.J., 2008. Chem. Rev. 108, 109–139.
Sorgenfrei, S., Chiu, C.Y., Gonzalez Jr, R.L., Yu, Y.-J., Kim, P., Nuckolls, C., Shepard, K.L., 2011. Nat. Nanotechnol 6, 126–132.
Stoeva, S.I., Lee, J.-S., Smith, J.E., Rosen, S.T., Mirkin, C.A., 2006. J. Am. Chem. Soc. 128, 8378–8379.
Shimron, S., Wang, F., Orbach, R., Willner, I., 2012. Anal. Chem. 84, 1042–1048.
Steel, A.B., Herne, T.M., Tarlov, M.J., 1998. Anal. Chem. 70, 4670–4677.
Turner, A.P.F., 2013. Chem. Soc. Rev. 42, 3184–3196.
Wu, D., Yin, B.C., Ye, B.C., 2011. Biosens. Bioelectron. 28, 232–238.
Wang, F., Elbaz, J., Orbach, R., Magen, N., Willner, I., 2011. J. Am. Chem. Soc. 133, 17149–17151.
Wang, J., Jiang, Y., Zhou, C., Fang, X., 2005. Anal. Chem. 77, 3542–3546.
Xiao, Y., Lou, X.H., Uzawa, T., Plakos, K.J.I., Plaxco, K.W., Soh, H.T., 2009. J. Am. Chem. Soc. 131, 15311–15316.

Xu, Q., Cao, A., Zhang, L.F., Zhang, C.Y., 2012. Anal. Chem. 84, 10845–10851.
Xia, F., White, R.J., Zuo, X.L., Patterson, A., Xiao, Y., Kang, D., Gong, X., Plaxco, K.W., Heeger, A.J., 2010. J. Am. Chem. Soc. 132, 14346–14348.
Xu, Q., Zhu, G., Zhang, C.Y., 2013. Anal. Chem. 85, 6915–6921.
Yin, B.C., Guan, Y.M., Ye, B.C., 2012. Chem. Commun. 48, 4208–4210.
Yuan, T., Liu, Z., Hu, L., Zhang, L., Xu, G., 2011. Chem. Commun. 47, 11951–11953.
Zuo, X., Xia, F., Xiao, Y., Plaxco, K.W., 2010. J. Am. Chem. Soc. 132, 1816–1818.
Zhang, B., Liu, B.Q., Tang, D.P., Niessner, R., Chen, G.N., Knopp, D., 2012. Anal. Chem. 84, 5392–5399.
Zhao, J., Chen, C., Zhang, L., Jiang, J., Yu, R., 2012. Biosens. Bioelectron. 36, 129–134.
Zhang, J., Song, S., Zhang, L., Wang, L., Wu, H., Pan, D., Fan, C., 2006. J. Am. Chem. Soc. 128, 8575–8580.
Zhou, Z., Du, Y., Dong, S., 2011. Anal. Chem. 83, 5122–5127.